Malaysian Journal
Of Civil Engineering

ENHANCED MESHFREE RPIM WITH NURBS BASIS FUNCTION FOR ANALYSIS OF IRREGULAR BOUNDARY DOMAIN

M.H. Mokhtaram[a*], M.A. Mohd Noor[a], M.Z. Jamil Abd Nazir[a], A.R. Zainal Abidin[a], A.Y. Mohd Yassin[b]

[a]School of Civil Engineering, Faculty of Engineering, Universiti Teknologi Malaysia, 81310 Skudai, Johor, Malaysia
[b]School of Energy, Geoscience, Infrastructure and Society, Heriot-Watt University Malaysia, 62200 Putrajaya, Malaysia

Article history
Received
09 January 2020
Received in revised form
05 February 2020
Accepted
10 February 2020
Published online
31 March 2020

*Corresponding author
mokhtazul@unisel.edu.my

Graphical abstract

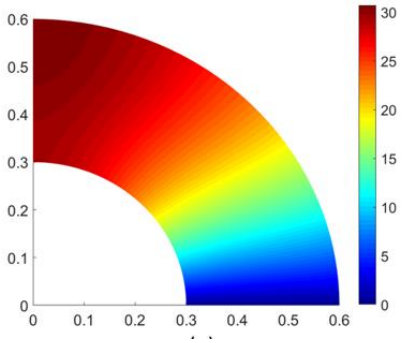

Abstract

Radial Point Interpolation Method (RPIM) has become a powerful tool to numerical analysis due to its ability to provide a higher-order approximation function with the Kronecker delta property, by which the field nodes can be fitted exactly. However, one of the major drawbacks of RPIM is the inefficiency in handling irregular domain problems. This paper presents an enhanced RPIM formulation that employs Non-Uniform Rational B-Splines (NURBS) basis functions to represent the exact geometry of the boundary domain. The NURBS is a mathematical model which provides an efficient and numerically stable algorithm to exactly represent all conic sections in engineering modelling. Taking advantage of the flexibility and adaptivity of RPIM approximation and the accuracy of geometric representations by NURBS, this new method is able to improve geometry accuracy and flexibility in numerical analysis, thus providing a better and more rational approach to analyze irregular domain problems. Numerical problem of steady heat transfer considering curved beam is presented to verify the validity and accuracy of the developed method. The essential boundary condition can simply be imposed using direct imposition as in Finite Element Method (FEM). The result shows that the RPIM/NURBS achieved the converged solution much faster than conventional RPIM and FEM, with the number of nodes required only less than 200 for an error of less than 0.01%. This shows the potential of the developed method as a powerful numerical technique for future development.

Keywords: Meshfree, RPIM, RBF Multi-quadratic, NURBS, Irregular domain

1.0 INTRODUCTION

Over the past several years, the meshfree method has become one of the most important methods in numerical analysis. The inventions of meshfree methods were motivated by the attempt to remove the need for predefined meshes which are required in Finite Element Method (FEM) thus attracted many researchers in their study. A meshfree method uses a pattern of nodes instead of mesh to discretize the domain. Ease in programming and no surface meshing, make these methods very attractive.

Construction of shape function is one of the most important and fundamental tasks in developing a meshfree method. The earliest work on meshfree shape function was Reproducing Kernel (RK) developed by Liu, et al. (1995, 1997). Afterwards, the Moving Least squares (MLS) have been used widely, such as Diffuse Element Method (DEM) (Nayroles, et al., 1992), Element-Free Galerkin (EFG) method (Belytscho, et al., 1994) and Meshless Local Petrov-Galerkin (MLPG) method (Atluri and Zhu, 1998). Although the meshfree methods is successfully applied, two major technical issues are still not properly solved. First, difficulties in the implementation of essential boundary condition. This is because of the approximation function does not possess Kronecker delta property. Second, the complexity involved in analysing irregular domains, where large numbers of

nodes are often required to capture adequately the geometry and this is the same issue faced by FEM.

A meshfree Point Interpolation Method (PIM) was proposed to address the first issue (Liu and Gui, 2001a, 2001b; Wang, et al., 2001). The PIM employed polynomials as its basis functions, in which the number of shape function is the same as the number of nodes. Hence, the PIM shape functions possess Kronecker delta property. However, PIM has weaknesses in which the moment matrix of the shape functions could be singular. Therefore special techniques are needed to overcome the issue. Wang and Liu (2002a, 2002b) proposed Radial Basis Functions (RBF) to overcome the singularity issue and termed as Radial PIM (RPIM). It has been proven that the moment matrix of RBF interpolations is invertible for constructing shape functions in PIM. The RPIM has recently made remarkable progress in the meshfree method of solutions. Its approximation function passes through each node point in the influence domain, thus makes the implementation of essential boundary conditions much easier and reducing complexity in numerical algorithms than other meshfree methods.

In highlighting the second issue, several studies have been made to improve the mapping process in numerical methods. One of the major studies was merging the analysis techniques with the predominant basis functions used in Computer-aided Design (CAD), namely Non-Uniform Rational B-Splines (NURBS). The NURBS basis function is a mathematical model, which provided an efficient and numerically stable algorithm that can exactly represent all conic sections and allows very flexible modelling. By manipulating the points and weights enables the flexible design of a great variety of geometric forms (Hughes, et al., 2005; Cottrell, et al., 2006; Bazilevs, et al., 2006). Among the earliest efforts to improve Rosolen and Arroyo (2013), who presented a couple of the Local Maximum Entropy Meshfree (LME) and NURBS (IGA-LME) through the imposition of reproducing conditions, made the mapping process in meshfree methods. Their work on infinite plate with circular hole shows that, the use of IGA-LME is significantly more accurate than conventional LME. Wang and Zhang, (2014), introduced a consistently coupled NURBS-reproducing kernel particle method (RKPM) with the aid of reproducing conditions to ensure consistency. The convergence behaviors are demonstrated for regular and irregular meshfree discretization. The results indicate that NURBS-RKPM can achieve a convergence rate that is very close to the exact solution. However, the non-interpolatory characters of the meshfree methods in their study, have made the continuation of the work more focused on improving the imposition of boundary conditions (Chi and Lin, 2016; Valizadeh, et al., 2015; Wang and Zhang, 2014). Therefore, taking advantage of the meshfree RPIM ability to fit the domain nodes exactly, the integration of RPIM with NURBS need to be explored and tested.

In this paper, the enhancement of RPIM analysis through integrating the formulations with NURBS basis functions have been proposed, which in the knowledge of this study, is the first-ever done thus improving the current issues of the meshfree method. To reinforce the idea of this developed method, studies have been conducted for two-dimensional (2D) planar analysis of steady heat transfer problem considering curved beam (quarter-ring) solid panel. The paper is organized as follows. A numerical model of 2D meshfree RPIM for steady heat transfer equation is first formulated based on the Garlekin Weighted-residual method (Garlekin WRM) using RBF Multi-quadrics (RBF-MQ) presented in section 2. An introduction of NURBS basis functions to construct the boundary of a domain is given in section 3. Section 4 reviews the formulation of the developed method and ways to integrate the RPIM and NURBS to achieve consistency. In section 5, numerical example considering curved beam is conducted to demonstrate the performance of the proposed method. Finally, the summary and conclusions of the proposed method given in section 6.

2.0 NUMERICAL MODEL OF MESHFREE RPIM FOR STEADY HEAT TRANSFER PROBLEM

Heat transfer is thermal energy in transit due to temperature differences. In civil engineering, it is widely used in studies related to fire protection of steel structures (Zhang, et al., 2016; Halverson, et al., 2005; Wong and Ghojel, 2003; Sakumoto, 1999).

The partial differential equation (PDE) of heat transfer can be expressed as below;

$$\frac{\partial}{\partial x}\left(k_x \frac{\partial U}{\partial x}\right) + \frac{\partial}{\partial y}\left(k_y \frac{\partial U}{\partial y}\right) = -q_H \tag{1}$$

where k_x and k_y are thermal conductivity in *x*-direction and *y*-direction, respectively. The equations can be written in matrix form as;

$$\{\partial\}[E]\{\partial\}^T U = -q_H \tag{2}$$

To obtain the Meshfree RPIM formulation, it is necessary to discretize the Equation (1) by Galerkin WRM. It starts with the construction of the shape functions first.

2.1 Formulation of RPIM Shape Functions

The shape functions should satisfy the following requirements (Liu, G.R., 2010). First, it should be sufficiently robust for arbitrarily distributed nodes; second, it should be stable; third, it should satisfy up to certain order of continuity; forth, it has to be supported compactly; finally, it should be computationally efficient. RBF-MQ as shown in equation (3) have been used to develop the RPIM shape functions in this study (Wendland, 1998).

$$R_i(x) = ({r_i}^2 + (\alpha_c d_c)^2)^q \tag{3}$$

where α_c and q are the dimensionless shape parameter and d_c is the characteristic length that relates to the nodal spacing in the domain of the point of interest x_Q. r_i is the distance between point of interest x_Q and a node at x_i defined as;

$$r_i = \sqrt{\left(x_Q - x_i\right)^2 + \left(y_Q - y_i\right)^2} \tag{4}$$

Consider a function $u(x)$ defined in the problem domain, Ω with a number of scattered field nodes. The field function is approximated as follows;

$$u(x) = \sum_{i=1}^{n} R_i(x) a_i = [R]^T \{\mathrm{a}\} \tag{5}$$

where *i* is the running index, $R_i(x)$ is a set of RBFs in the space coordinates $x = (x, y)$, n is the number of RBFs determined by the number of nodes in the domain. Thus, the coefficients a_i can be determined by enforcing equation (5) to be satisfied at the nodes in the domain by evaluating the equation subsequently at each node point. The matrix form of these equations can be expressed as;

$$[R_n]\{\mathrm{a}\} = \{U\} \tag{6}$$

where $\{U\}$ is the vector of nodes values in the domain, $[R_n]$ is the moment matrix of RBFs and $\{\mathrm{a}\}$ is the vector of unknown coefficient which can be solved as;

$$\{\mathrm{a}\} = [\mathrm{R}_n]^{-1}\{U\} \tag{7}$$

By substituting equations (7) into equations (5), the function of $u(x)$ can be re-written as;

$$u(x) = [R]^T [\mathrm{R}_n]^{-1}\{U\} \tag{8}$$

Finally, $[R]^T[\mathrm{R}_n]^{-1}$ is the matrix of RPIM shape functions, ϕ.

2.2 Discretization of Steady Heat Transfer by Galerkin WRM

Substituting equation (8) into equation (2) obtain the following;

$$\{\partial\}[E]\{\partial\}^T\{\phi\}\{U\}^T \neq -q_H \tag{9}$$

To obtain sufficient number of equations, by following the procedure of Galerkin WRM, multiply equation (9) with the vector of shape function $\{\phi\}$ then integrate over influence domain to produce sufficient number of independent equations as shown below;

$$\int_{\Omega} \{\phi\}^T (\{\partial\}[E]\{\partial\}^T\{\phi\}\{U\}^T + q_H) d\Omega = 0 \tag{10}$$

To relax the continuity requirement, integration by parts (IBP) can be employed for equation (10). The following result are obtained;

$$\int_{\Omega} \{\phi\}^T\{\partial\}[E]\{\partial\}^T\{\phi\}\{U\}^T d\Omega = \tag{11}$$

$$\int_{\Omega} \{\phi\}^T q_H d\Omega + \int_{s} \{\phi\}^T\{b\}^T ds$$

Having established this, equation (11) is the discretized or weak-formed of steady heat transfer equation. It can be expressed in matrix form as;

$$[K]\{U\}^T = \{q\} + \{b\} = \{R\} \tag{12}$$

where,

$$[K] = \int_{\Omega} \{\phi\}^T\{\partial\}[E]\{\partial\}^T\{\phi\} d\Omega \tag{13}$$

$$\{q\} = \int_{\Omega} \{\phi\}^T q_H d\Omega \tag{14}$$

$$\{b\} = \int_{s} \{\phi\}^T\{b\}^T ds \tag{15}$$

The corresponding matrix $[K], \{U\}$ and $\{R\}$ are known as the stiffness matrix, vector of degree of freedom (DOF), and load vector respectively for numerical model of steady heat transfer problems.

3.0 FORMULATION OF NURBS BASIS FUNCTION

NURBS is generally defined by its order, control points, weights associated with control points and knot vectors. NURBS's first principle is from the Bezier curve then B-Splines has been derived from the Bezier curve and NURBS from B-Splines. A Bezier curve is an approximating curve, where the control points are unable to be interpolated but only approximated. However, the algorithms of Bezier curves get numerically unstable with an increasing number of control points. Thus, Bezier's formulation was extended to B-Splines to facilitate these limitations.

3.1 B-Splines Basis Function

Based on knot vector and polynomial order, B-Splines basis function $N_{i,p}$ are computed using Cox-de-Boor recursion formula as shown in equation (16) for p =0 and equation (17) for p =1,2,3,… *n*.

$$N_{i,0}(\xi) = \begin{cases} 1, & \text{if } \xi_i \le \xi < \xi_{i+1} \\ 0, & \text{otherwise} \end{cases} \tag{16}$$

$$N_{i,p}(\xi) = \frac{\xi - \xi_i}{\xi_{i+p} - \xi_i} N_{i,p-1}(\xi) \tag{17}$$

$$+\frac{\xi_{i+p+1}-\xi}{\xi_{i+p+1}-\xi_{i+1}}N_{i+1,p-1}(\xi)$$

3.2 NURBS Basis Function

A piecewise polynomial parametrization of a circle cannot be covered by B-Splines basis functions. However, by weighing, w_i the B-Splines basis functions, it received a rational basis functions, known as NURBS which preserve all properties of B-Splines. Therefore, the NURBS basis function in one parametric direction can be expressed as below;

$$R_i^p(\xi)=\frac{N_{i,p}(\xi)w_i}{\sum_{i=1}^{n}N_{i,p}(\xi)w_i} \tag{18}$$

A NURBS surface is more or less the same thing only in two directions. It is computed by the tensor product of NURBS basis functions in two parametric dimensions ξ and η. It is defined by a net of $n\times m$ control points, two knot vector Ξ and $\mathcal{H}$, two polynomial degrees p and q, and correspondingly the basis functions $N_{i,p}(\xi)$ and $M_{j,q}(\eta)$. Finally, the equations of NURBS basis function in two parametric directions and the NURBS surface can be expressed as in equation (19) and (20) respectively;

$$R_{i,j}^{p,q}(\xi,\eta)=\frac{N_{i,p}(\xi)M_{j,q}(\eta)w_{i,j}}{\sum_{i=1}^{n}\sum_{j=1}^{m}N_{i,p}(\xi)M_{j,q}(\eta)w_{i,j}} \tag{19}$$

$$S^n(\xi,\eta)=\sum_{i=1}^{n}\sum_{j=1}^{m}R_{i,j}^{p,q}(\xi,\eta)\,\boldsymbol{B_{i,j}} \tag{20}$$

4.0 INTEGRATED FORMULATION OF MESHFREE RPIM AND NURBS BASIS FUNCTION

In the proposed method, the NURBS basis functions was used to describe the boundary of the problem domain and the meshfree discretization, a set of points inside the boundary, will be created for construction of the RPIM approximation function.

The use of NURBS basis functions introduces the concept of parametric space. The parametric space is a pre-image of the NURBS mapping and needs to be presented as a unit square through appropriate normalisation. The parametric space is defined as $\widehat{\Omega}=[0,1]$ with an associated set of parametric coordinates $(\hat{\xi},\hat{\eta})\in\widehat{\Omega}$. However, to adapt the new concept of parametric space, the additional mapping must be performed. As illustrated in Figure 1, two mapping are considered; a mapping $\phi^e\colon\widetilde{\Omega}\longrightarrow\widehat{\Omega}^e$ and $F\colon\widehat{\Omega}\rightarrow\Omega$. The mapping $x^e\colon\widetilde{\Omega}\longrightarrow\Omega^e$ is given by the composition $F\circ\phi^e$.

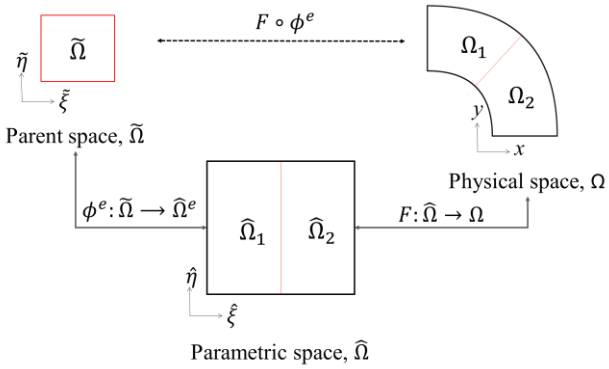

Figure 1 Spaces and mapping transformations in NURB basis function

4.1 Mapping Transformations

The parametric space requires an additional mapping to allow operations in the parent space coordinates. The mapping from the parametric space to the physical space, $F\colon\widehat{\Omega}\rightarrow\Omega$, can be written as;

$$x^e(\tilde{\xi})=\sum_{j=1}^{n}R_j(\phi^e(\tilde{\xi}))B_j \tag{21}$$

where R_j denote the shape functions by NURBS basis functions, B_j is the control point and ϕ^e is the shape function by polynomial functions for four-node rectangular element.

4.2 Numerical Integration

The integrals over the physical space are split into element integrals with a domain denoted by Ω_e. These integrals are transferred to the parametric space $\widehat{\Omega}$ through a geometrical mapping and then to the parent space $\widetilde{\Omega}$ through affine mapping, where the numerical integration is actually performed. With these final mappings, it is possible to integrate a function $f\colon\Omega\longrightarrow\mathbb{R}$ over the physical space as;

$$\begin{aligned}\int_{\Omega}f(x,y)d\Omega&=\sum_{e=1}^{n}\int_{\Omega_e}f(x,y)d\Omega_e\\&=\sum_{e=1}^{n}\int_{\widehat{\Omega}_e}f\left(x(\hat{\xi}),y(\hat{\eta})\right)|J_{\hat{\xi}}|d\widehat{\Omega}_e\\&=\sum_{e=1}^{n}\int_{\widetilde{\Omega}_e}f(\tilde{\xi},\tilde{\eta})|J_{\tilde{\xi}}||J_{\tilde{\xi}}|d\widetilde{\Omega}_e\end{aligned} \tag{22}$$

where $|J_{\hat{\xi}}|$ is the Jacobian determinant of geometrical mapping, and $|J_{\tilde{\xi}}|$ is the Jacobian determinant of affine mapping. The Jacobian determinant can be defined as;

$$|J_\xi| = \frac{\partial(x,y)}{\partial(\xi,\eta)} = \begin{vmatrix} \frac{\partial x}{\partial \xi} & \frac{\partial x}{\partial \eta} \\ \frac{\partial y}{\partial \xi} & \frac{\partial y}{\partial \eta} \end{vmatrix} = \frac{\partial x}{\partial \xi}\frac{\partial y}{\partial \eta} - \frac{\partial x}{\partial \eta}\frac{\partial y}{\partial \xi} \quad (23)$$

5.0 NUMERICAL EXAMPLE

Here, numerical examples are presented to evaluate the performance of the developed RPIM considering the NURBS integration approach for the analysis of steady heat transfer problem. Curved beam (quarter-ring) is chosen to examine the ability of the developed method in dealing with irregular domains. The geometrical parameters are provided as illustrated in Figure 2. The boundary conditions are adopted as T is 0 on Γ_3 and q is 0 on Γ_1, Γ_2 and Γ_4, where T is the temperature and q is the heat generation respectively. The material parameters used are given in Table 1.

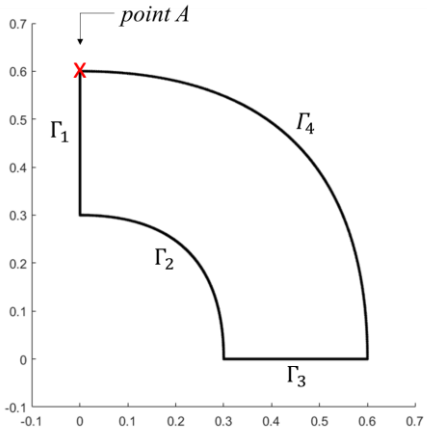

Figure 2 Domain of the problem

Table 1 Input material parameters

Material parameters	
Thermal conductivity, k_x	400 W/mK
Thermal conductivity, k_y	400 W/mK
Internal heat generation, q_H	50 W/m^3
Thickness of element, t	0.1 m

5.1 Geometry of the Problem Domain

The problem domain was modelled by determining how many elements are needed. It shows that, one direction of the problem domain is curved while the other direction is a straight feature. Therefore, the lowest polynomial order of p = 1 in $\hat{\xi}$-direction and q = 2 in $\hat{\eta}$-direction can be used. For comparison, two types of models are to be built based on the order elevation and knot insertion as shown in Table 2. The control points and associated weight are listed in Table 3.

Table 2 Type of models

Models	-direction	Poly. order	Control point	Knot Vectors	Total control Point $(n \times m)$
A	$\hat{\xi}$	p = 2	n = 3	Ξ ={0,0,0,1,1,1}	9
	$\hat{\eta}$	q = 2	m = 3	H={0,0,0,1,1,1}	
B	$\hat{\xi}$	p = 2	n = 4	Ξ ={0,0,0,0.5,1,1,1}	12
	$\hat{\eta}$	q = 2	m = 3	H={0,0,0,1,1,1}	

Table 3 Control points and weighting

Model A		Model B	
Control points	Weighting	Control points	Weighting
(0.3, 0)	1	(0.3, 0)	1
(0.3, 0.3)	$1/\sqrt{2}$	(0.3, 0.1243)	$(1+1/\sqrt{2})/2$
(0, 0.3)	1	(0.1243, 0.3)	$(1+1/\sqrt{2})/2$
(0.45, 0)	1	(0, 0.3)	1
(0.45, 0.45)	$1/\sqrt{2}$	(0.45, 0)	1
(0, 0.45)	1	(0.45, 0.1864)	$(1+1/\sqrt{2})/2$
(0.6, 0)	1	(0.1864, 0.45)	$(1+1/\sqrt{2})/2$
(0.6, 0.6)	$1/\sqrt{2}$	(0, 0.45)	1
(0, 0.6)	1	(0.6, 0)	1
		(0.6, 0.2485)	$(1+1/\sqrt{2})/2$
		(0.2485, 0.6)	$(1+1/\sqrt{2})/2$
		(0, 0.6)	1

Figure 3 shows the NURBS basis function for all models. The new knot value would have to be inserted with multiplicities equal to one, to define new elements across whose boundaries functions will be C^{p-1}-continuity. By repeating the existing knot values, it reduces the continuity of the basis function across existing element boundaries. Figure 4 shows the physical geometry of the models.

5.2 Creation of Nodes in spaces

The first step in defining the process of mapping transformation is to create nodes in parent space, $(\tilde{\xi}, \tilde{\eta})$. Then followed by a node in the parametric space, $(\hat{\xi}, \hat{\eta})$. The coordinate transformation using the polynomial functions for four-node rectangular element. Once the parametric space is defined, then the NURBS basis function can be compute. However, the NURBS basis function are weighted B-Splines with weighted control points, therefore, B-Splines will be computed first as shown in Figure 3 by using equation (17). Then, The NURBS basis functions are computed by weighting the B-splines basis functions using equation (18). Finally, the coordinate transformation of parametric space to physical space can be performed through equation (21). Figure 5 shows the coordinate transformation from parent space to physical space. For Model B (refer to Figure 5 (b)), nodes 5, 10, 15, 20 and 25 in the physical space are the result of the assembly nodes of the elements in the parametric space

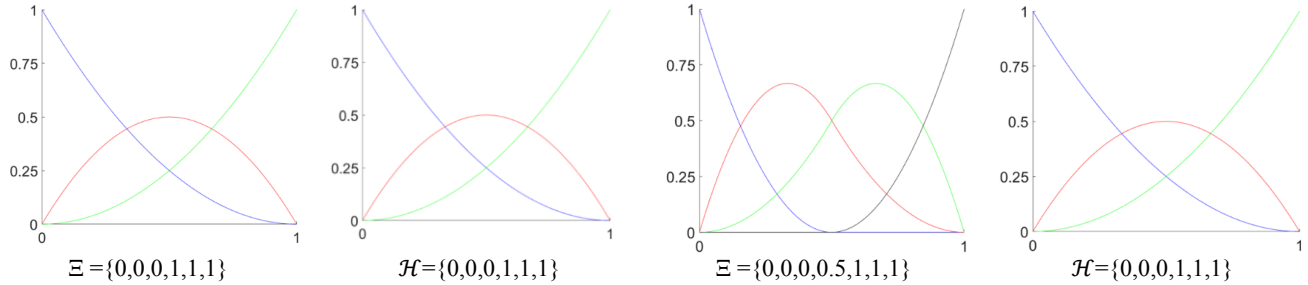

Figure 3 NURBS basis function for (a) Model A and (b) Model B

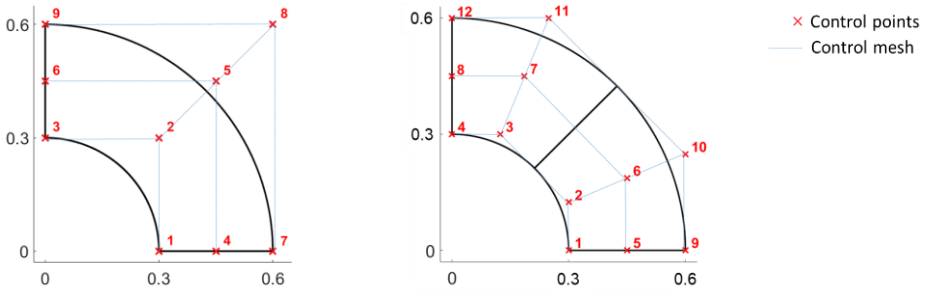

Figure 4 Physical geometry of the problem domain for (a) Model A and (b) Model B

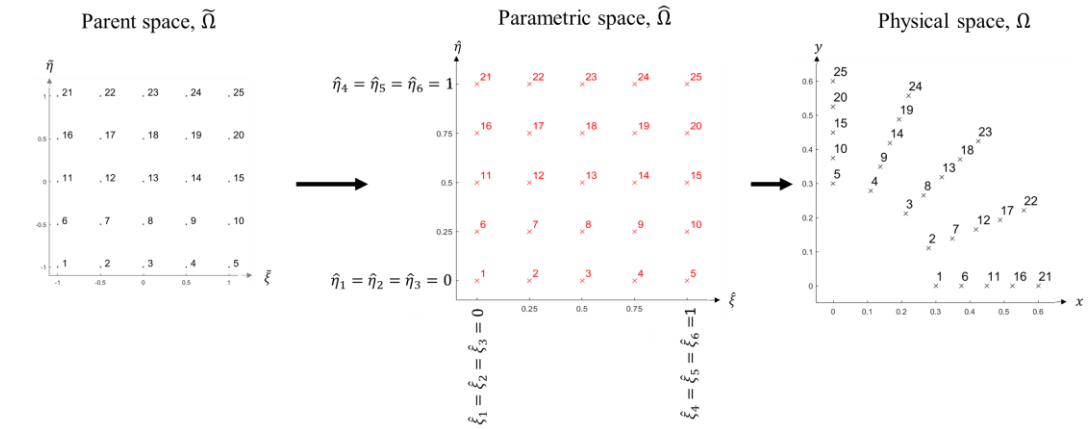

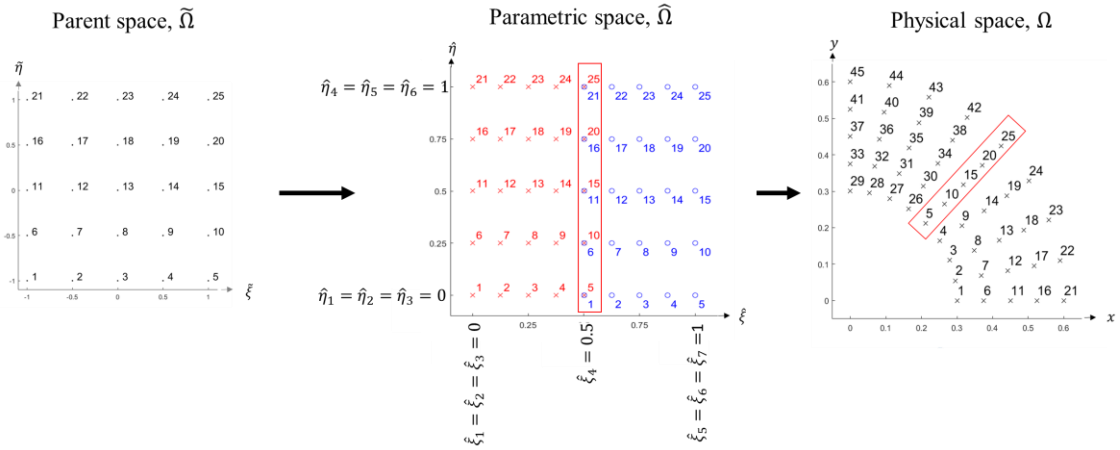

Figure 5 Coordinate transformation for (a) Model A and (b) Model B

5.3 Meshfree RPIM and NURBS approximations

The solution of the numerical model is conducted in parent space, therefore, equation (12) than becomes.

$$[K] = \sum_{k}^{n_c} \sum_{i=1}^{n_g} \widetilde{w}\{\phi\}^T\{\partial\}[E]\{\partial\}^T\{\phi\}\left|J_{\tilde{\xi}}\right|\left|J_{\tilde{\xi}}\right| \quad (24)$$

$$\{q\} = \sum_{k}^{n_c} \sum_{i=1}^{n_g} \widetilde{w}\{\phi\}^T q_H\left|J_{\tilde{\xi}}\right|\left|J_{\tilde{\xi}}\right| \quad (25)$$

where n_c and n_g is the number of parent spaces and gauss quadrature, respectively and $\widetilde{w}$ is the gauss weight. For stiffness matrix, ϕ is the derivatives of RPIM shape functions with respect to parent space, $\tilde{\Omega}$. Therefore, it must be expressed in terms of parametric space, $\hat{\Omega}$ and physical space, Ω. Hence, by the chain rule of partial differentiation, equation (24) than becomes.

$$[K] = \sum_{k}^{n_c} \sum_{i=1}^{n_g} \widetilde{w}[B]^T[E][B]\left|J_{\tilde{\xi}}\right|\left|J_{\tilde{\xi}}\right| \quad (26)$$

where,

$$[B] = J_{\tilde{\xi}}^{-1}(J_{\tilde{\xi}}^{-1}\begin{Bmatrix}\frac{\partial\phi}{\partial\xi}\\ \frac{\partial\phi}{\partial\eta}\end{Bmatrix}) \quad (27)$$

$J_{\tilde{\xi}}$ and $J_{\tilde{\xi}}$ are the Jacobian matrix of polynomial functions for four-node rectangular element and NURBS basis function, respectively.

$\left|J_{\tilde{\xi}}\right|$ and $\left|J_{\tilde{\xi}}\right|$ are the Jacobian determinant of $J_{\tilde{\xi}}$ and $J_{\tilde{\xi}}$ respectively. The $\left|J_{\tilde{\xi}}\right|$ is calculated for affine mapping, which is the isoparametric concept. This is because of the domains of parent and parametric spaces are usually in the particular forms of rectangular. Then, the $\left|J_{\tilde{\xi}}\right|$ is calculated for geometrical mapping of the problem domain.

5.4 Imposition of Boundary Condition and solution of the simultaneous equation

In the proposed method, shape functions constructed possesses the Kronecker delta property, where the approximation satisfies the values of variables at field nodes. This property of shape function enables direct imposition of boundary conditions.

Finally, the problem is ready to be solved. The solution of the matrix equation is represented as;

$$[K]\{\widetilde{U}\} = \{R\}$$
$$\{\widetilde{U}\} = [K]^{-1}\{R\}$$
$$\{\widetilde{U}\} = [K]\backslash\{R\} \quad (28)$$

6.0 RESULTS AND DISCUSSION

Point A shown in Figure 2 is used as a reference point. Since there are no closed-form solution available for the example given, the "exact" solution herein is defined from a FEM commercial software that is COMSOL, with a very fine mesh. The optimum values of the parameters are obtained as the lowest range of values of the error at point A. Based on previous research recommendations (Liu and Gu, 2005; Wang and Liu, 2002b; Liu et. al., 2005; Liu, 2010), suggested values of shape parameters RBF-MQ are q =0.98 and α_c=3.

6.1 Effect of the Knot Insertion on Parametric Space

The convergence of the temperature error with an increasing number of nodes at point A achieved by models A and B is shown in Figure 6.

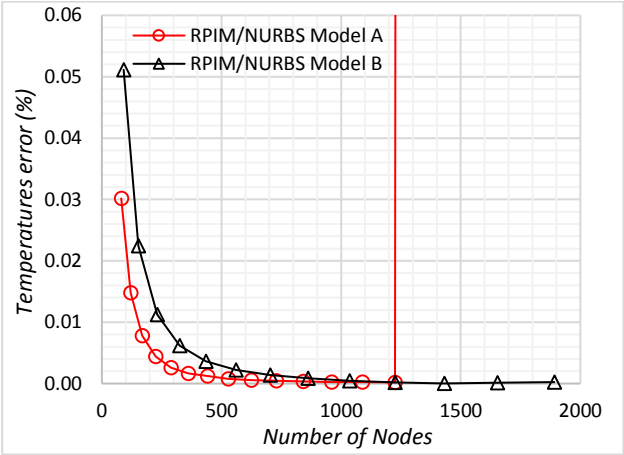

Figure 6 Convergence rate of for Model A (1 knot span) and Model B (2 knot span) at point A

The figure shows that, both models would provide a converged solution if the number of nodes is taken over 500. It also shows that Model A give better convergence compared to Model B. However, for Model A, a sudden jump of error is obtained when the number of the nodes becomes large. Therefore, to keep a balance between accuracy and stability, Model B is used for the next analysis.

6.2 Convergence Study

Comparison is made by comparing their convergence rate of area for the developed method against each other. The evenly distributed 6, 15 and 66 nodes plotted against the number of Gauss points have been studied as shown in Figure 7. The figure shows that, this method is able to provide an almost exact area with very few numbers of nodes and Gauss points.

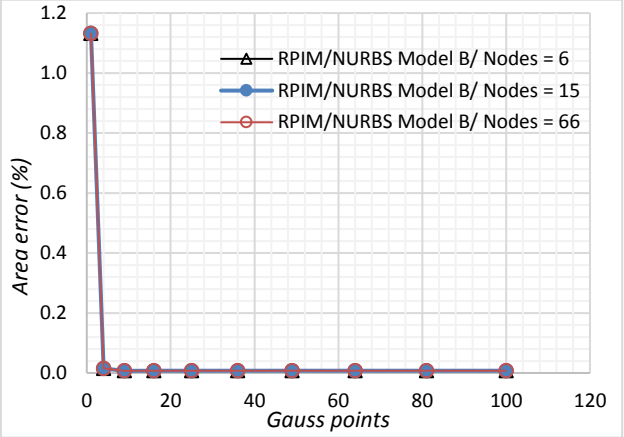

Figure 7 Convergence of area error

As this study focuses on new formulation, the main interest is to compare the performance of the developed method against the conventional RPIM and the established numerical methods, FEM. Figure 8 shows the comparison of their convergence rate of area.

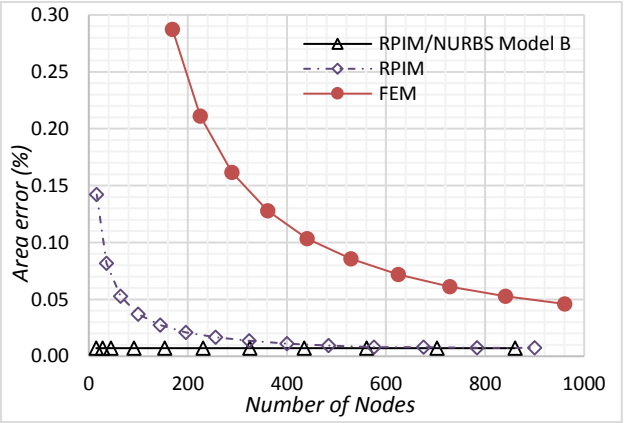

Figure 8 Convergence of area error for RPIM/NURB Model B, RPIM and FEM

Based on Figure 8, RPIM/NURBS and RPIM show that both methods can provide an area very close to the exact area. However, with the aid of NURBS, RPIM is able to provide the exact area with very few nodes. While FEM requires many nodes to get better convergence rate. This is due to the mesh concept in FEM.

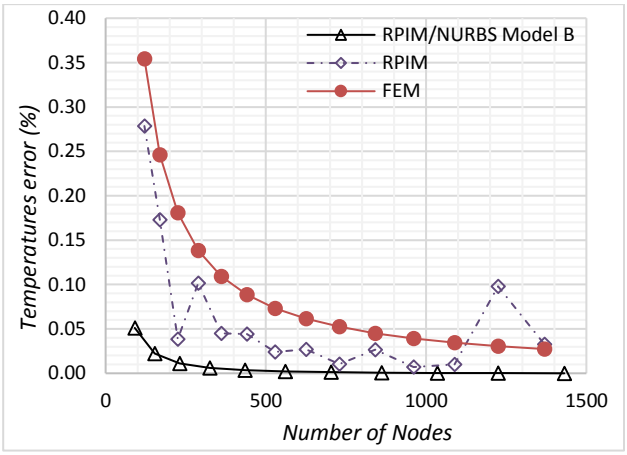

Figure 9 Convergence rate of temperatures

Figure 9 shows the convergence of the temperatures error with an increasing number of nodes. Based on the figure, it clearly shows that the RPIM/NURBS performs the best convergence compared to conventional RPIM and FEM. The RPIM/NURBS achieved an almost exact solution with the number of nodes required only less than 200 for an error of less than 0.01%. The convergence of conventional RPIM is difficult to achieve, where a sudden jump of error is obtained when the number of the nodes grows. Therefore, the idea of enhanced RPIM with NURBS has proven to improve the performance of conventional RPIM as well as the numerical analysis. Figure 10 shows the temperature fields comparisons between RPIM/NURBS and COMSOL software.

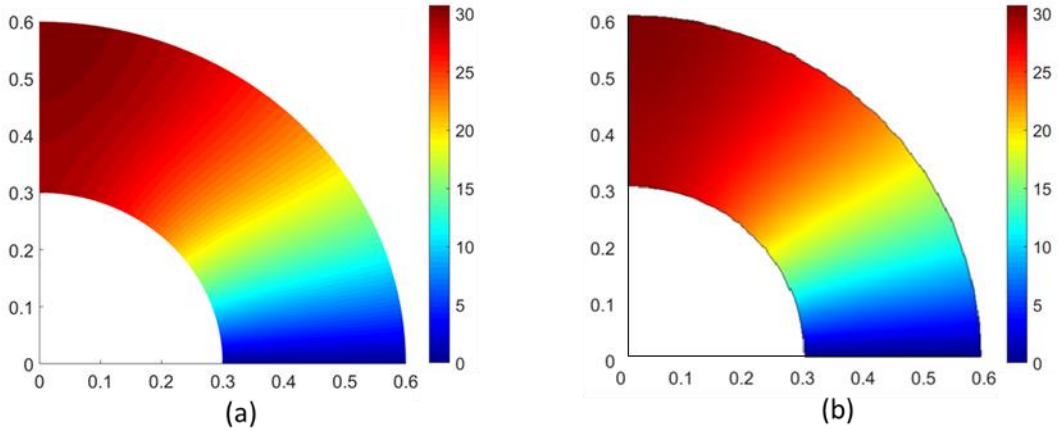

Figure 10 Comparison of the temperature fields (a) RPIM/NURBS Model B and (b) COMSOL software

7.0 CONCLUSIONS

In this paper, the concept of integrating on the modelling of the exact geometry through the NURBS basis functions and the analysis of the model using RPIM method are presented and discussed in a step-by-step manner. The RPIM method constructed based on a Galerkin formulation with the adoption of RBF to produce the shape functions and then followed by the integration of NURBS basis function into the RPIM method. The developed method improves on the existing techniques in the following ways. Since the variables are approximate using RPIM that poses kronecker delta properties, the imposition of the essential boundary condition can be simply imposed using direct imposition. In addition, the geometric exactness of the proposed method can be achieved regardless of the order of continuity and consistency of the approximation to perform the analysis.

The method was applied to a steady heat transfer with irregular domain (curved beam) problem and RBF-MQ has been used as the basis function. The irregularity of the domain has been beneficial in highlighting the advantages of the proposed method. Verifications of the problem has been compared with conventional RPIM and FEM with a very fine mesh. The first comparison is the convergence rate of area, where the developed method is able to provide an exact area with very few numbers of nodes and Gauss points. Second is the convergence rate of the temperature error where it yielded better result and shows excellent agreement for all test cases. Such verifications give a confirmed level of confidence and validate the use of the developed method as new technique in numerical analysis.

Acknowledgements

The authors acknowledge the members of the Malaysian Society for Numerical Methods (MSNM), for assisting the computer algorithm development and Universiti Teknologi Malaysia (UTM) for the financial support through Geran Universiti Penyelidikan (GUP) vote number 19H41 for this research.

References

[1] Atluri, S. N. and Zhu, T. 1998. A new meshless local Petrov-Galerkin (MLPG) Approach In Computational Mechanics. *Computational Mechanics*. 22: 117-127.

[2] Bazilevs, Y., Beirao, L., Veiga, D., Cottrell, J., Hughes T.J.R., and Sangalli, G. 2006. Isogeometric Analysis: Approximation, Stability And Error Estimates For H-Refined Meshes. *Mathematical Models and Methods in Applied Sciences*. 16: 1031-1090.

[3] Belytscho, T., Lu, Y.Y. and Gu, L. 1994. Element-free Galerkin methods. *International Journal for Numerical Methods in Engineering*. 37: 229-256.

[4] Chi, S.W. and Lin, S.P. 2016. Meshfree Analysis With The Aid Of NURBS Boundary. *Computational Mechanics*. 58: 371–389.

[5] Cottrell, J.A., Reali, A., Bazilevs, Y. and Hughes, T.J.R. 2006. Isogeometric analysis of structural vibrations. *Computer Methods in Applied Mechanics and Engineering*. 195: 5257-5296.

[6] Greco, F., Coox, L., Maurin, F. and Desmet, W. 2017. NURBS-enhanced maximum-entropy schemes. *Computer Methods in Applied Mechanics and Engineering.* 317: 580–97.

[7] Halverson, H., Bausano, J., Case, S. and Lesko, J. 2005. *Simulation of Structural Response of Composite Structures under Fire Exposure*. Department of Engineering Science & Mechanics at Blacksburg, Virginia Tech.

[8] Hughes, T.J.R., Cottrell, J.A., and Bazilevs, Y. 2005. Isogeometric analysis: CAD, finite elements, NURBS, Exact Geometry And Mesh Refinement. *Computer Methods in Applied Mechanics and Engineering*. 194: 4135–4195.

[9] Liu, G.R., Zhang, G.Y., Gu, Y.T., and Wang, Y.Y., 2005. A Meshfree Radial Point Interpolation Method (RPIM) For Three-Dimensional Solids. *Computational Mechanics*. 36: 421-430.

[10] Liu, G.R. 2010. Meshfree methods: Moving beyond the Finite Elements Method. 2nd ed., CRC Press, Florida.

[11] Liu, G.R. and Gu, Y.T. 2001a. A Point Interpolation Method For Two-Dimensional Solids. *International Journal for Numerical Methods in Engineering*. 50: 937-951.

[12] Liu, G.R. and Gu, Y.T. 2001b. A Local Radial Point Interpolation Method (LR-PIM) For Free Vibration Analyses of 2-D solids. *Journal of Sound and Vibration*. 246(1): 29-46.

[13] Liu, G.R. and Gu, Y.L 2005. An Introduction To Meshfree Methods And Their Programming. Springer, Netherlands.

[14] Liu, W. K., Jun, S., Li, S., and Zhang, Y.F. 1995. Reproducing kernel particle methods. *International Journal for Numerical Methods in Fluids*. 20: 1081-1160.

[15] Liu, W. K., Li, S. F., and Belytschko, T. 1997. Moving least-square reproducing kernel methods (I) Methodology and convergence. *Computer Methods in Applied Mechanics and Engineering*. 143: 113–154.

[16] Nayroles, B., Touzot, G. and Villon, P. 1992. Generalizing the finite element method: diffuse approximation and diffuse elements. *Computational Mechanics*. 10: 307-318.

[17] Rosolen, A. and Arroyo, M. 2013. Blending Isogeometric Analysis And Local Maximum Entropy Meshfree Approximants. *Computer Methods in Applied Mechanics and Engineering.* 264: 95–107.

[18] Sakumoto, Y. 1999. Research on New Fire-Protection Materials and Fire-Safe Design. *Journal of Structural Engineering*. 125(12): 1415-1422.

[19] Valizadeh, N., Bazilevs, Y., Chen, J.S. and Rabczuk, T.A. 2015. Coupled IGA–Meshfree Discretization Of Arbitrary Order Of Accuracy And Without Global Geometry Parameterization. *Computer Methods in Applied Mechanics and Engineering*. 293: 20–37.

[20] Wang, D. and Zhang, H. 2014. A consistently coupled isogeometric–meshfree method. *Computer Methods in Applied Mechanics and Engineering*. 268: 843–870.

[21] Wang, J. G., Liu, G. R., and Wu, Y. G. 2001. A Point Interpolation Method for Simulating Dissipation Process of Consolidation *Computer Methods in Applied Mechanics and Engineering.* 190: 5907-5922.

[22] Wang, J. G., & Liu, G. R. 2002a. A Point Interpolation Meshless Method Based On Radial Basis Functions. *International Journal for Numerical Methods in Engineering*. 54(11): 1623-1648.

[23] Wang, J. G., & Liu, G. R. 2002b. On the Optimal Shape Parameters Of Radial Basis Functions Used For 2-D Meshless Methods. Computer Methods In Applied Mechanics And Engineering. 191(23): 2611-2630.

[24] Wang, Q., Zhou, W., Cheng, Y., Ma, G., Chang, X. and Chen, E. 2018. NE-IIBEFM for Problems With Body Forces: A Seamless Integration of The Boundary Type Meshfree Method and the NURBS boundary in CAD. *Advances in Engineering*. 118: 1-17.

[25] Wendland, H. 1998. Error Estimates For Interpolation By Compactly Supported Radial Basis Functions Of Minimal Degree. *Journal of Approximation Theory*. 93: 258–396.

[26] Wong, M.B., and Ghojel, J.I. 2003. Sensitivity Analysis of Heat Transfer Formulations for Insulated Structural Steel Components. *Journal of Fire Safety*. 38: 187-201.

[27] Zhang, C., Silva, J.D., Weinschenk, C., Kamikawa, D., and Hasemi, Y. 2016. Simulation Methodology for Coupled Fire-Structure Analysis: Modeling Localized Fire Tests on a Steel Column. *Fire Technology*. 52: 239–262.

[28] Zhang, H., and Wang, D. 2017. Reproducing kernel formulation of B-spline and NURBS basis functions: a meshfree local refinement strategy for isogeometric analysis. *Computer Methods in Applied Mechanics and Engineering*. 320: 474–508.